Two-Degree-of-Freedom Admittance-type Droop Control for Plug-and-Play DC Microgrid

Zheming Jin, Josep M. Guerreros
Department of Energy Technology
Aalborg University
Aalborg, Denmark
zhe@et.aau.dk

***Abstract*—For DC microgrids, the "plug and play" capability is one of the most desired functionalities to formulate a fully flexible and scalable system. The "plug and play" operation will put twofold requirements on the control of power sources: on the one hand, they shall share the load properly; on the other hand, the system stability shall be ensured. In this paper, a two degree-of-freedom admittance-type droop control method is proposed to fulfill the requirements of the "plug and play" operation. In the proposed method, both conventional proportional power sharing function and virtual inertia injection capability are included to provide an integrated decentralized solution to ensure proper power sharing and system stability, and therefore being helpful to achieve "plug and play" DC microgrid.**

Keywords—DC microgrids, plug and play, virtual inertia, stability, droop control.

I. INTRODUCTION

Microgrids, as small-scaled power systems with generation, consumption and storage packed as entity are now becoming the ideal candidate of building block of future smart grid [1-3]. DC microgrids are now drawing great attention due to their convenience and efficiency in integrating renewable energy sources, energy storage systems and supporting modern electronic end-user loads (e.g., LEDs, electronics and motor drives), especially in off-grid and islanded applications, such as data centers, telecommunication stations, future self-sustaining buildings, more-electric aircrafts and ships [4-5].

The scalability and "plug and play" capability is usually considered as one of the major advantage of DC microgrid over its AC counterpart. The "plug and play" operation of DC microgrids requires that a proper power sharing among power sources (i.e. power converters) shall be maintained or be rebuilt automatically at all cases, including the case that one or more power sources are newly plugged in or switched off. At the same time, the stability of the microgrid shall be ensured during this process. Nevertheless, when a new power source is plugged in, the existing communication infrastructure (e.g., the communication link or protocol) may not be able to adaptively exchange information with the new power source. Therefore, a decentralized control solution is preferred in this case.

In DC microgrids, the conventional droop method is widely used as the primary control level to ensure a proper power sharing among paralleled power sources [3,6,7]. Droop method is firstly developed to achieve fully decentralized coordination of paralleled power modules in telecommunication industry. To a certain extent, the droop control method can provide "plug and play" functionality. However, it is noteworthy that droop method is focusing on ensuring a proportional steady-state power sharing according to the rating of power sources. In addition to that, the system stability issue is not taken into consideration due to the fact that the method is firstly designed for modular power supply, in which the power supplies have the same parameters in controller and passive components. Nevertheless, in DC microgrids, one of the major feature is that not only power sources are interfaced by power converters but also the majority of the loads, which leads to significant constant power load (CPL) instability issue (i.e. negative incremental resistance issue) of the system, which is mandatory to be considered when designing the control method.

In [8], the impact of controllers on achieving droop control is analyzed. The results show that even with the same droop coefficient, different controller will lead to significant different transient response. Meanwhile, it is also proven that current control based droop controllers will have a faster response and better stability margin than the conventional voltage control based droop controllers. In the author's previous work [9], the inertia issue of DC microgrids is analyzed, and the virtual inertia injection is proposed as a mean to enhance the transient response of the system response in transient states. However, the major problem of the previous work is that it focused on smooth transient response, but the potential distribution of virtual capacitor is not considered. In this paper, a two-degree-of-freedom admittance-type droop control method is proposed to provide a decentralized solution for combined power sharing and stability enhancement. In the proposed method, conventional droop method is included as the first degree-of-freedom to ensure proper power sharing, while virtual inertia is used as the second degree-of-freedom to manage the system stability and also for differential transient power sharing for an autonomous power sharing purpose.

In the following parts of this paper, the requirement of PnP operation is firstly analyzed from the perspective of immitance characteristic. The limitation of operational voltage range is considered in addition to the conventional stability criterion. Secondly, the principle of proposed two-degree-of-freedom droop method is detailed. An analytical model of the proposed

method is proposed to analyze its behavior with different settings of two droop coefficients. Finally, several simulations are carried out using PLECS, the proposed method using both symmetrical design or asymmetrical design methods are validated. The results show improved transient response during ON/OFF control and load changing.

II. Operational Requirement of Plug and Play

A. Constant Power Load Instability Issue

For the constant power nature of tightly controlled point of load converters, the following expression will be satisfied within the control bandwidth of the controller:

$$i_{Load} = \frac{P_{Load}}{V_{dc}} \tag{1}$$

where V_{dc}, i_{Load}, and P_{Load} are the bus voltage, input current and power of the point of load converter (as CPL).

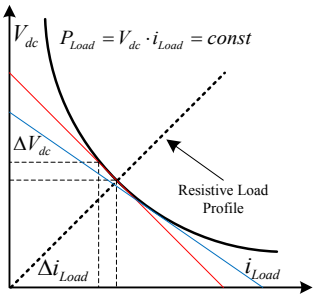

Fig. 1. Negative impedance behavior of CPLs.

As shown in Fig. 1, the negative incremental resistance of a CPL can be calculated by:

$$\frac{\partial V_{dc}}{\partial i_{Load}} = \frac{\partial}{\partial i_{Load}}\left(\frac{P_{Load}}{i_{Load}}\right) = -\frac{P_{Load}}{i^2_{Load}} = -\frac{V^2_{dc}}{P_{Load}} = R_{CPL} \tag{2}$$

It shows that the CPLs, although still consuming power, are performing a negative resistance to the system, which reduce the damping and affects the stability. A linearized small-signal analytical model of CPL can be derived by (2), which contains the calculated negative resistance as well as a controlled current source. In addition to that, due to the limited control bandwidth of controller, the practical CPL will also show frequency-dependent impedance characteristic above the control bandwidth. From impedance based analysis, stability of the bus voltage is determined by:

$$V_{dc}(s) = \frac{V_{ref} Z_{CPL}(s)}{Z_o(s) + Z_{CPL}(s)} = V_{ref} T_m(s) \tag{3}$$

$$T_m(s) = \frac{1}{1 + Z_o(s)/Z_{CPL}(s)} \tag{4}$$

where $V_s(s)$, $Z_o(s)$ and $Z_{CPL}(s)$ stand for source voltage, source-side output impedance and negative impedance of CPLs, all presented in frequency-domain transfer functions. $T_m(s)$ is the minor loop gain of the system, which is critical to the system stability analysis [8-11].

The sufficient condition of system stability is that all the dominant poles of $T_m(s)$ locate in the stable region. It requires the source-side output impedance to have smaller magnitude than the negative impedance, or at least fulfill the marginal stability condition. In Fig.2, a generalized scenario of CPL stability issue in droop-controlled DC microgrid is illustrated by bode diagram.

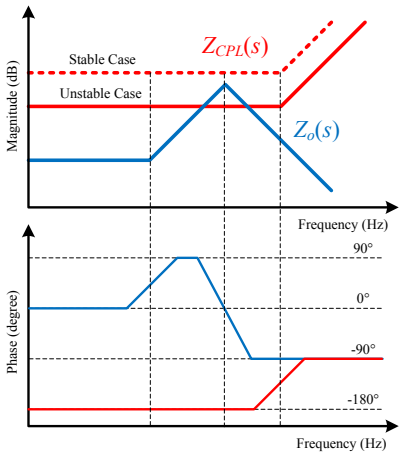

Fig. 2. Generalized frequency response of analytical CPL stability issue.

B. Requirement Due to Steady-state Voltage Drop

In DC microgrids, the virtual resistance based droop control method, of which control principle can be formulated as shown in (5), is the most common method to coordinate several paralleled power sources. Under normal circumstances, the design of droop coefficient is determined by the maximum voltage droop divided by the maximum output current of the converter, which can be further formulated as shown in (6) using a quantified maximum voltage drop factor δ.

$$V_{dc} = V_{ref} - I_o R_d \tag{5}$$

$$V_{\min} = (1-\delta)V_{ref} = V_{ref} - I_{o\max} R_d = V_{ref} - \frac{P_{\max}}{(1-\delta)V_{ref}} R_d \tag{6}$$

With equation (6), the maximum load power for droop control method can be derived as:

$$P_{Load} \le P_{\max} = (1-\delta)\delta \frac{V^2_{ref}}{R_d} \tag{7}$$

By combining equation (7) with (2), the impedance characteristic based stability margin in case of steady-state (i.e., the case that $s \to 0$) can be derived as:

$$\left.\frac{|Z_o(s)|}{|Z_{CPL}(s)|}\right|_{s\to 0} = \frac{|R_d|}{|R_{CPL}|} \le \frac{\delta}{1-\delta} \tag{8}$$

In (8), the operational voltage range requirement of the DC microgrid is presented as a criterion of steady-state impedance

matching issue. For example, impedance difference more than 19.1dB is required to ensure a voltage drop factor below δ=10%, or 25.6dB for δ=5%.

C. Requirement due to Small-signal Voltage Stability

To ensure system stability, the minor loop gain formulated in (4) can not have any right-hand-pole, more conservatively, it means the magnitude of source-side output impedance shall be smaller than the input impedance of loads (i.e. equivalent negative impedance of CPLs) for all frequency components which is referred as Middlebrook stability criterion.

The source-side output impedance is mostly determined by the controller of power source. Generally, the steady-state value (i.e., $Z_o(s)$ with $s \to 0$) of source-side output impedance is dominant by the droop coefficient, whereas the peak value is determined by the controller behavior and will always appear in high frequency range.

For PnP operation of DC microgrids, the load power will be uncertain, at the same time, the control bandwidth of load converter is unpredictable. Therefore, a worst case shall be considered, in which the control bandwidth of CPL could be very high or even infinite. In addition to that, some stability margin will be mandatory, e.g., the Middlebrook stability criterion suggests that a stability margin over 6dB is needed. Therefore, a new constrain of source-side output impedance can be derived from (8):

$$\left|Z_o(s)\right\|_{peak} \le \frac{1-\delta}{2\delta}\left|Z_o(s)\right\|_{s\to 0} = \frac{1-\delta}{2\delta}R_d \qquad (9)$$

Equation (9) suggests that the difference between the peak value of source-side output impedance and its steady-state value shall be limited below a certain threshold, which is determined by the voltage drop factor of the system design. For example, impedance difference below 13dB is required to ensure the system will always have enough damping for a voltage drop factor of δ=10%, or 19.5dB for δ=5%.

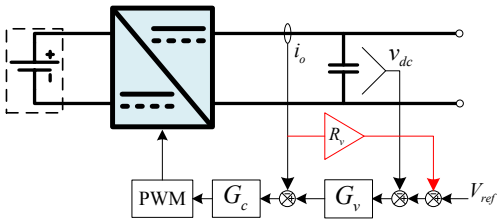

(a) Control diagram of impedance-type droop controller

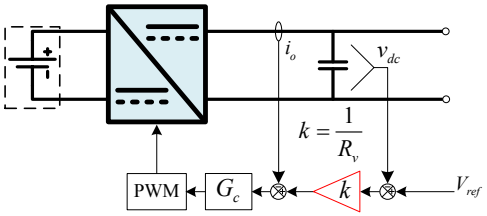

(b) Control diagram of admittance-type droop controller

Fig. 3. Different realization methods of droop control

III. Proposed Two-Degree-of-Freedom Admittance-Type Droop Method

A. Advantages of Admittance-type Droop Controller

In Fig.3, the different control architectures for both more conventional impedance-type droop controller and admittance-type droop controller are shown. In [8], the difference between these two major types of realization methods are analyzed. As a major conclusion, the admittance-type droop controller will perform a minimized delay and leads to reduced peak value of source-side output impedance. For example, the analytical results of a study case microgrid are shown in Fig.4 and Fig.5. In the study case, the inner current loops are simplified as first-order delay with a control bandwidth ω_c=1500 rad/s, and droop coefficients are set to be 0.1Ω for both converters. In the impedance-type controller the voltage PI controller has a proportional term equal to 0.5 and an integral term equal to 300. The DC capacitance is assumed to be 1.1mF.

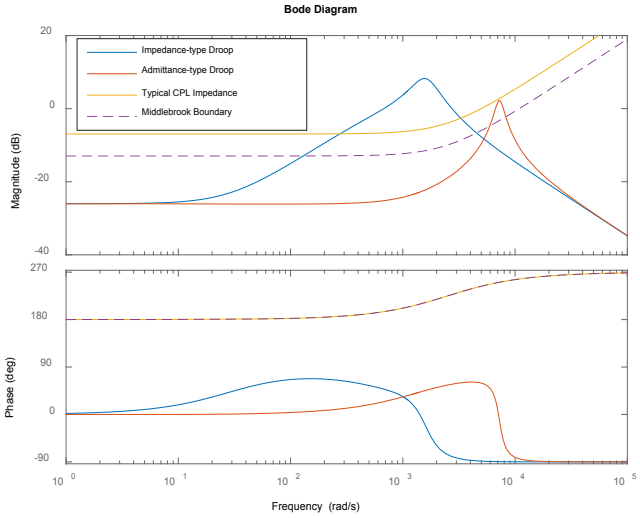

Fig. 4. Frequency response of source-side output impedance

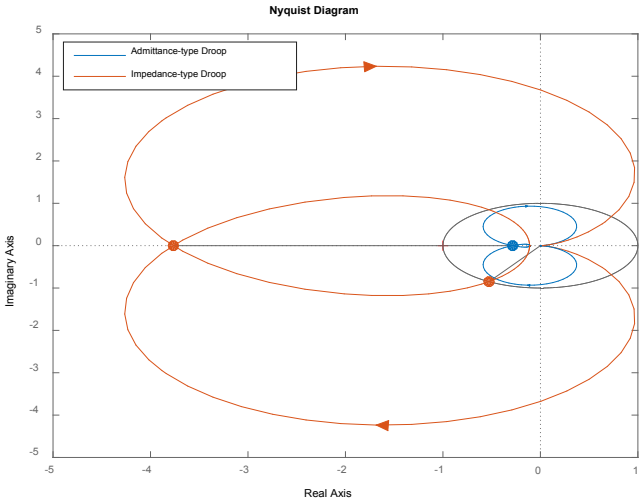

Fig. 5. Nyquist diagram of the system's minor loop gain

In this study case, the CPL is set to be a critical case for $\delta=10\%$. In both Fig.4 and Fig.5, the admittance-type controller shows more desirable impedance characteristic and stability margin. In Fig.5, the Nyquist diagram shows that admittance-type controller can still ensure a stable operation while impedance-type controller can not. However, it is also shown that the stability margin is quite limited and more conservative stability criterion (e.g., the boundary of Middlebrook criteria shown in Fig.4) is still offended.

B. *Impact of Virtual Capacitor on System Stability*

To enhance the stability margin of the system (e.g., the study case shown in the previous section), the most straight forward method is to add additional capacitor to the DC bus. As a result, it will directly reduce the peak value of the source-side output impedance and reduce the frequency where the peak value appears. However, the increased DC capacitance will also increase the cost and bring more challenging issue to the protection of the DC microgrid. Meanwhile, the reduction of the frequency where the peak value appear may also limit the damping effect due to the fact that the input impedance of CPL can decrease in a lower frequency range (as shown in Fig.6(a)). In the previous work presented in [9], the capacitive virtual component is proposed to introduce virtual inertia to the system, and therefore to improve the transient response of the system. In Fig.6(b), the source-side output impedance with additional virtual capacitor. From the analytical results, the major difference between using virtual capacitor and real capacitor is that using virtual capacitor does not change the frequency where the peak value appear, at the same time, the damping effect is also slightly better, which is analyzed in the following section. An analytical model for the proposed method is established in detail in the following parts of this section.

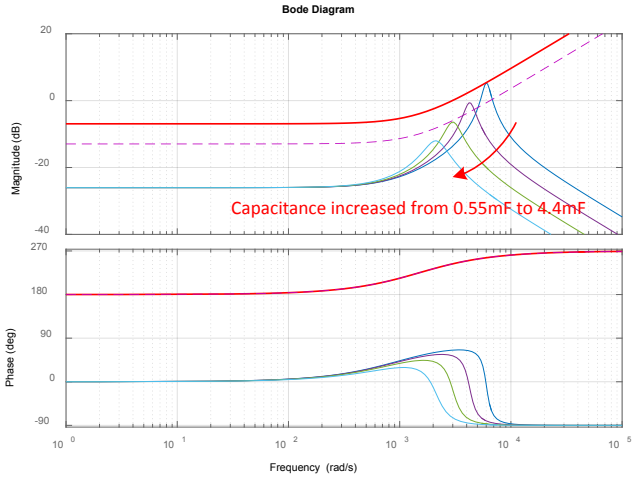

(a) Output Impedance with increased DC capacitance.

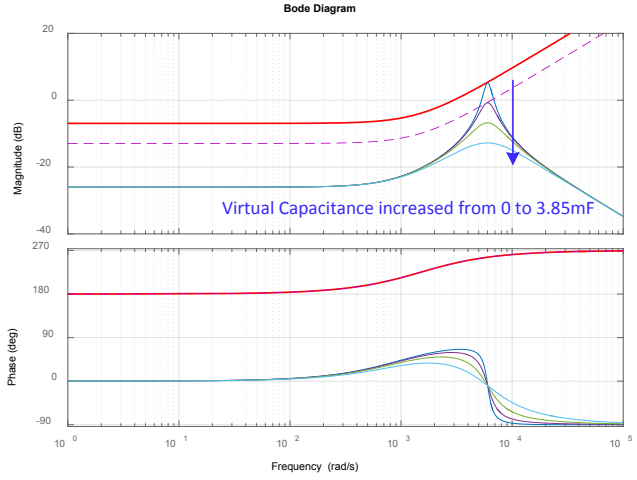

(b) Output Impedance with increased virtual capacitance.

Fig. 6. Frequency response of source-side output impedance

C. *Two-degree-of-freedom Droop Method and Its Analytical Model*

For an admittance-type droop controller, the droop function is achieved by the finite gain behavior, which can be detailed by the following function:

$$i_o^{ref}(s)=\frac{1}{R_d}\left(u_{no}-u(s)\right) \tag{10}$$

Similarly, the behavior of capacitive virtual component can be descripted as:

$$i_o^{ref}(s)=sC_v\left(u_{no}-u(s)\right) \tag{11}$$

A major feature of admittance-type droop controller is that adding additional component to the droop coefficient will result in paralleled virtual component, which make it feasible for introducing additional degree-of-freedom. In the previous section, the impact of virtual capacitor on system stability is analyzed. As a conclusion, with increased capacitance (either real or virtual capacitance), the peak value of the source-side output impedance can be reduced, and the stability margin of the system will be improved correspondingly. With properly designed capacitive virtual component, the system will be able to fulfill the conservative requirement of PnP operation discussed in the Section II.C. In addition to that, it is also noteworthy that the virtual capacitance will not affect the steady-state power sharing effect, because in steady states $s\rightarrow 0$. For this reason, the two degree-of-freedoms which are the resistive and capacitive virtual components can be designed independently. By combining (10) and (11), the control function of the proposed method can be presented by:

$$i_o^{ref}(s)=\left(\frac{1}{R_d}+sC_v\right)\left(u_{no}-u(s)\right)=Y_d(s)\left(u_{no}-u(s)\right) \tag{12}$$

When adopting the proposed two-degree-of-freedom droop method, the conventional resistive component will dominant the steady-state response as a result of its decisive effect on the source-side output impedance in the low frequency-range. It will therefore determine the steady-state power sharing effect as it did in the conventional droop method. At the same time, capacitive virtual component will determine the converter's characteristic in transient-states, and enhance the stability of the system. However, it is noteworthy that the virtual capacitor used in the proposed method does not affect the steady-state power sharing of the system, and therefore, they can be distributed in a different way other than the conventional

method that design the virtual components by the power rating of the converter. In this case, the virtual capacitor as the second degree-of-freedom of the proposed method can also be used to differentiate the dynamic response of power sources in transient states according to their different characteristics of generation (e.g., costs and dynamics).

The dynamic power sharing of proposed method can be analyzed using the analytical model of output impedance. For the proposed method, the resistive and capacitive components can be treated separately by assuming that the output current is within the operational range of the converter and the inner current loop is simplified as a first-order delay. Therefore, the two-parts of output impedance can be descripted using the following equations:

$$i_o(s)=\left(\frac{1}{R_d}+sC_v\right)\left(u_{no}-u(s)\right)G_{clc}(s)=i_o^R(s)+i_o^C(s) \quad (13)$$

$$i_o^R(s)=\frac{1}{R_d}\left(u_{no}-u(s)\right)G_{clc}(s)=Y_{conv}^R(s)\left(u_{no}-u(s)\right) \quad (14)$$

$$i_o^C(s)=sC_v\left(u_{no}-u(s)\right)G_{clc}(s)=Y_{conv}^C(s)\left(u_{no}-u(s)\right) \quad (15)$$

where $G_{clc}(s)$ is the close-loop transfer function of the whole current loop.

When assuming the bandwidth of $G_{clc}(s)$ is ω_{clc}, the admittance term in (14) and (15) can be calculated as shown in the following equation:

$$\begin{cases} Y_{conv}^R(s)=\dfrac{1}{R_d}G_{clc}(s)=\dfrac{1}{s\,R_d/\omega_{clc}+R_d} \\ Y_{conv}^C(s)=sC_vG_{clc}(s)=\dfrac{sC_v\omega_{clc}}{s+\omega_{clc}} \end{cases} \quad (15)$$

$$\begin{cases} Z_{conv}^R(s)=\dfrac{1}{Y_{conv}^R(s)}=s\,R_d/\omega_{clc}+R_d \\ Z_{conv}^C(s)=\dfrac{1}{Y_{conv}^C(s)}=\dfrac{1}{C_v\omega_{clc}}+\dfrac{1}{sC_v} \end{cases} \quad (16)$$

Based on (16), the analytical equivalent circuit of the proposed method can be derived as shown in Fig.7. It shows that the virtual capacitive component will perform an equivalent RC circuit (which is a typical damper circuit for CPL instability problem), and therefore providing additional damping effect when compared to real capacitors (as shown in Fig.6.).

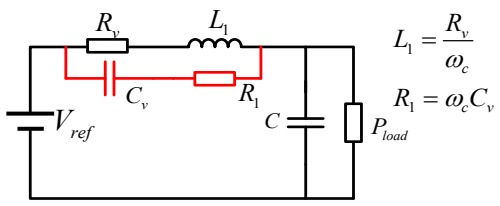

Fig. 7. Analytical equivalent circuit for the propose control method

IV. Simulation Validation

To validate the proposed method, a study case microgrid is simulated using PLECS. The study case is composed by two Buck converters, a programmable load performing CPL, as illustrated in Fig.8. The parameters of simulation are listed in Table I.

Two different simulation scenarios are simulated to validate the proposed method. In the first simulation scenario, the stability enhancement effect of the introduction of the second degree-of-freedom (i.e., the capacitive virtual component) are tested and compared with more conventional droop method with only resistive virtual component. In addition to that, an additional comparison between the symmetrical distribution and asymmetrical distribution of virtual capacitors is carried out to show the potential of using the second degree-of-freedom for dynamic power sharing purpose.

In the second simulation scenario, the PnP operation of DC microgrid with proposed method is tested. In this scenario, an additional power source is plugged into the DC microgrid, and then the converter #2 is switched off. The performance of ON/OFF control is tested in this simulation scenario.

TABLE I. Parameters of Simulated Study Case

Description of the Parameter	*Symbol*	*Value*
Global No-load Voltage Reference	V_{ref}	115 V
Source Voltage	E_1, E_2	230 V, 230 V
Inductance of Buck Converters	L_1, L_2	8 mH, 8 mH
Stary Resistance of inductors,	r_1, r_2	0.1 Ω, 0.1 Ω
Switching Frequency	f_{sw}	10 kHz
Virtual Resistances for Droop Control	R_{d1}, R_{d2}	0.5 Ω, 0.5 Ω
Total Capacitance in DC Bus	C	0.55 mF
Proportion Term of Current Controller	K_{pc1}, K_{pc2}	0.035, 0.035
Integral Term of Current Controller	K_{ic1}, K_{ic2}	10, 10
Load Power	P_{CPL}	4800W (1600W/step)

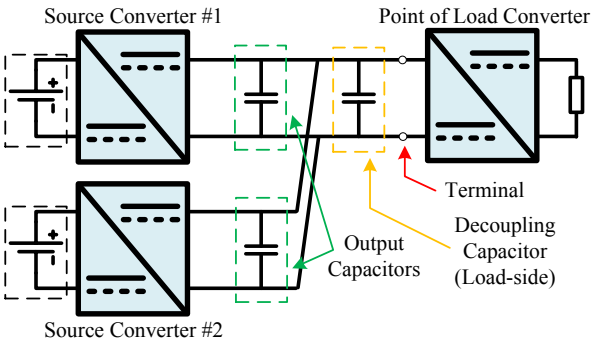

Fig. 8. Illustartion of simulated study case.

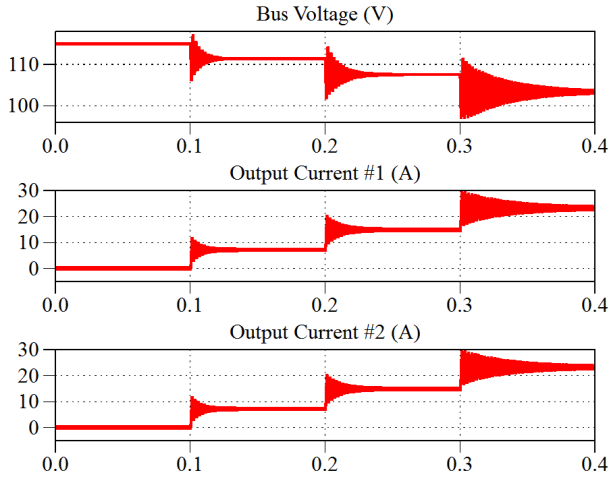

Fig. 9. Simulation results using only the admittance-type controller with $R_{d1}=R_{d2}=0.5\Omega$, $C_{v1}=C_{v2}=0$.

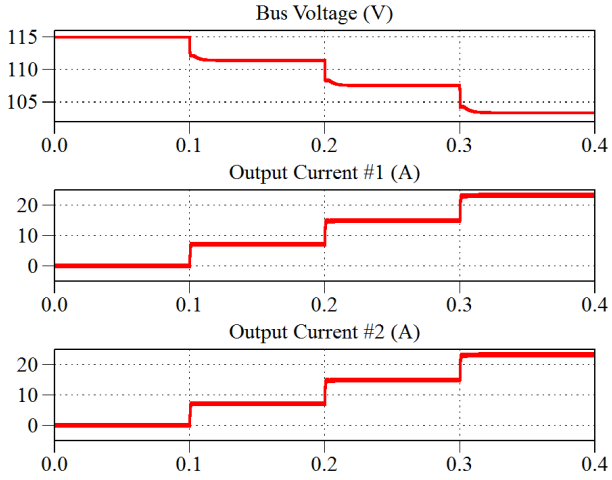

Fig. 10. Simulation results using proposed method with $R_{d1}=R_{d2}=0.5\Omega$, $C_{v1}=C_{v2}=3.5C=1.925mF$.

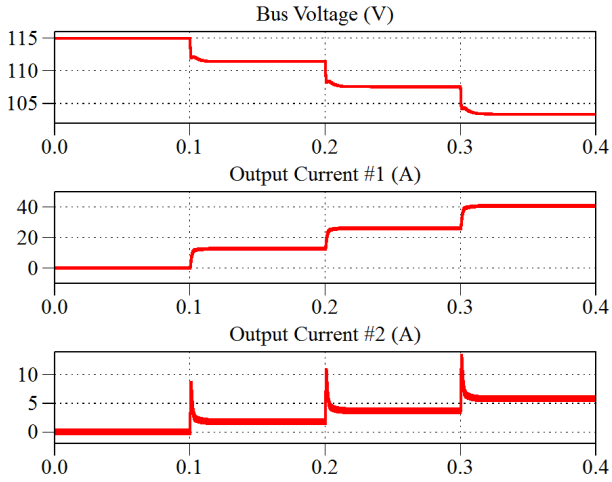

Fig. 11. Simulation results using proposed method with $R_{d1}=0.285\Omega$, $R_{d2}=2\Omega$, $C_{v1}=0, C_{v2}=7C=3.85mF$.

In Fig.9, the simulation results using only the resistive admittance-type controller is presented, it can be seen from the simulation results that the system stability margin is quite limited, and the transient response is poor. In Fig.10, the simulation results using the proposed method with virtual capacitor set to $C_{v1}=C_{v2}=3.5C=1.925mF$ is presented. Compared with the simulation results shown in Fig.9, the system stability damping is significantly improved. In Fig. 11, the setting of droop coefficients are both changing into an asymmetrical combination. In this simulation, the steady-power sharing is changed into $R_{d1}:R_{d2}=1:7$, while the virtual capacitor setting is changed into $C:C_{v1}:C_{v2}=1:0:7$. In this case, the converter #1 contribute more to the steady-state power, but does not contribute to the system stability enhancement. As a result, a differentiated dynamic power sharing can be seen from the simulation results shown in Fig.11. It indicates that the use of second degree-of-freedom can also contribute to the dynamic power management approaches to achieve a characteristic based power sharing of different kinds of power sources.

In Fig.12 and Fig.13, the simulation results of the second scenario is presented. In this simulation scenario the ON/OFF process of PnP operation is simulated. During the time period between 0 to 0.4s, the study case DC microgrid is loaded with programmable load. At t=0.4s, an additional converter is plugged into the system. At t=0.8s, the converter #2 is switched off and fully disconnected by open the connecter. In this case the DC capacitor is no longer connected to the DC bus which results in a reduction that half the DC capacitance.

In Fig.12, the simulation results by using only the admittance-type droop controller is presented. The simulation results indicate that although the converter #3 can be plugged

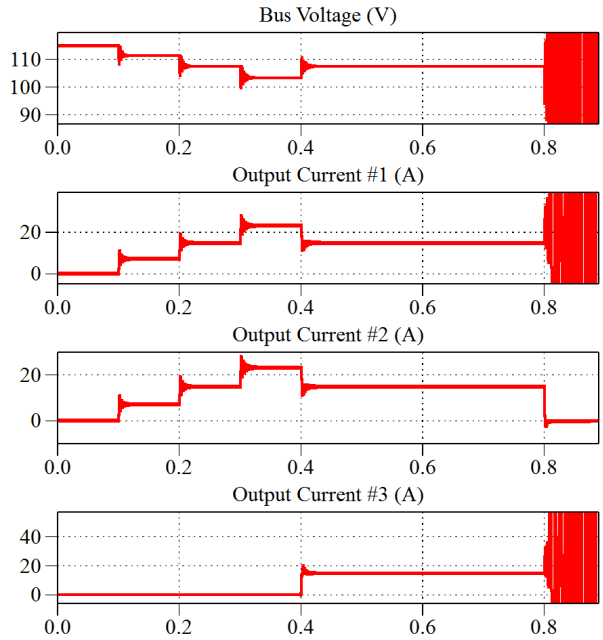

Fig. 12. Simulation results using only admittance-type droop controller with $R_{d1}=R_{d2}=0.5\Omega$, $C_{v1}=C_{v2}=0$.

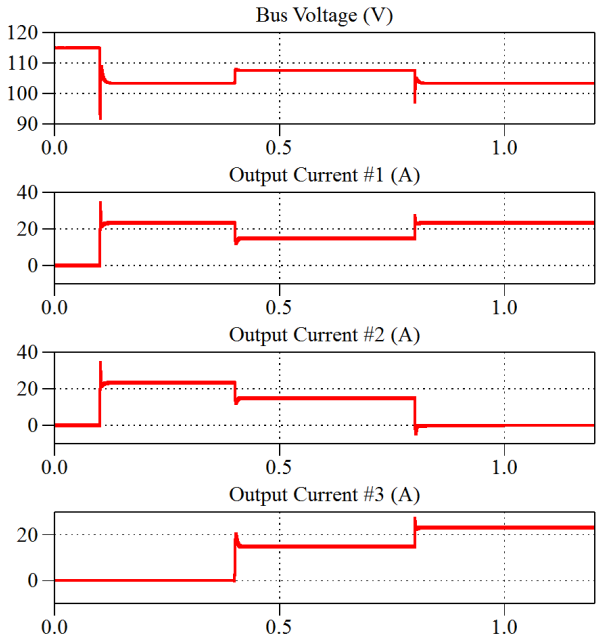

Fig. 13. Simulation results using proposed method with $R_{d1}=R_{d2}=0.5\Omega$, $C_{v1}=C_{v2}=3C=1.65mF$.

in and share the load with existing converters properly, the system will not be able to maintain stable operation once the converter #2 is switched off.

In Fig.13, the simulation results using proposed method is shown. Several noteworthy modifications can be seen from the simulation results. Firstly, 0 to100% load step of constant power load can be accepted when using proposed control method, while the conventional method can not maintain stable due to a large-signal stability issue. Secondly, similar to the simulation results shown in Fig.11, the system damping is improved significantly when compared with more conventional method. Nevertheless, the system maintains stable operation after the converter #2 is switched off at t=0.8s with a disconnection of half of the DC capacitance.

The simulation results show that with the proposed control method, the PnP operation including plug-in and switch-off can be ensured and the stability of the system is significantly improved.

V. CONCLUSION

In this paper, a two-degree-of-freedom admittance-type droop control method is proposed to fulfill the requirement of PnP operation for DC microgrids. The conventional virtual resistance is included as the first degree-of-freedom to ensure proper power sharing in steady-state, at the same time, capacitive virtual component is proposed to be used as the second degree-of-freedom to ensure system stability and damping. The requirement of PnP operation is analyzed from perspective of source-side impedance. The principle of proposed method and its analytical model is proposed. Simulations are carried out using PLECS and the simulation results show that with proposed method the stability margin and the system damping can be significantly improved. In addition to that the stability during PnP operation including plug-in and switch-off with some capacitance changing can be ensured.

REFERENCES

[1] Lasseter, Robert H., and Paolo Paigi. "Microgrid: A conceptual solution." In *Power Electronics Specialists Conference, 2004. PESC 04. 2004 IEEE 35th Annual*, vol. 6, pp. 4285-4290. IEEE, 2004.

[2] B. T. Patterson, "DC, Come Home: DC Microgrids and the Birth of the "Enernet"," in IEEE Power and Energy Magazine, vol. 10, no. 6, pp. 60-69, Nov.-Dec. 2012.

[3] J. M. Guerrero, J. C. Vasquez, J. Matas, L. G. De Vicuña, and M. Castilla, "Hierarchical control of droop-controlled AC and DC microgrids - A general approach toward standardization," *IEEE Trans. Ind. Electron.*, vol. 58, no. 1, pp. 158–172, 2011.

[4] Rosero, J. A., J. A. Ortega, E. Aldabas, and L. A. R. L. Romeral. "Moving towards a more electric aircraft." *IEEE Aerospace and Electronic Systems Magazine* 22, no. 3 (2007): 3-9.

[5] Z. Jin, L. Meng, J. M. Guerrero and R. Han, "Hierarchical Control Design for Shipboard Power System with DC Distribution and Energy Storage aboard Future More-Electric Ships," in *IEEE Transactions on Industrial Informatics*, vol. PP, no. 99, pp. 1-1.

[6] F. Gao *et al.*, "Comparative Stability Analysis of Droop Control Approaches in Voltage-Source-Converter-Based DC Microgrids," in *IEEE Transactions on Power Electronics*, vol. 32, no. 3, pp. 2395-2415, March 2017.

[7] F. Chen, R. Burgos and D. Boroyevich, "Output impedance comparison of different droop control realizations in DC systems," *2016 IEEE 17th Workshop on Control and Modeling for Power Electronics (COMPEL)*, Trondheim, 2016, pp. 1-6.

[8] Z. Jin, L. Meng and J. M. Guerrero, "Comparative admittance-based analysis for different droop control approaches in DC microgrids," *2017 IEEE Second International Conference on DC Microgrids (ICDCM)*, Nuremburg, 2017, pp. 515-522.

[9] Z. Jin, L. Meng, R. Han, J. M. Guerrero and J. C. Vasquez, "Admittance-type RC-mode droop control to introduce virtual inertia in DC microgrids," *2017 IEEE Energy Conversion Congress and Exposition (ECCE)*, Cincinnati, OH, USA, 2017, pp. 4107-4112.

[10] J. Sun, "Impedance-Based Stability Criterion for Grid-Connected Inverters," in *IEEE Transactions on Power Electronics*, vol. 26, no. 11, pp. 3075-3078, Nov. 2011.

[11] A. Riccobono and E. Santi, "Comprehensive Review of Stability Criteria for DC Power Distribution Systems," in *IEEE Transactions on Industry Applications*, vol. 50, no. 5, pp. 3525-3535, Sept.-Oct. 2014.